



A two-electrode frequency-scan system for gesture recognition*

Gang Ma^a, Haofeng Chen^{a,b}, Peng Wang^b, Shuai Dong^a, Xiaojie Wang^{a,b,*}

^a Department of Precision Machinery and Precision Instrumentation, University of Science and Technology of China, Hefei, Anhui, 230026, China

^b Institute of Advanced Manufacturing Technology, Hefei Institutes of Physical Science, Chinese Academy of Sciences, Changzhou, Jiangsu, 213164, China



ARTICLE INFO

Associate Editor: Prof Bin Yao

Keywords:

Bio-impedance measurement
Gesture recognition
Frequency-scan
Feature extraction

ABSTRACT

In this paper, we proposed a novel two-electrode, frequency-scan gesture recognition system based on bio-impedance measurement. This method not only achieves a high accuracy in recognizing common gestures and pinch gestures, but also reduces the measurement complexity and the number of electrodes. We developed a bespoke circuit with two medical electrodes to collect data from the back of the hand and presented a frequency-scan method to increase the diversity of impedance data. Feature extraction method was adapted to explore the representative features for gesture recognition, and machine learning classification models with five-fold cross-validation were used to train and realize accurate gesture recognition. To verify the effectiveness of this system, we designed two groups of nine gestures in a hand-gesture recognition experiment. The results showed that the system achieved a recognition accuracy of 98.3% with a group of four common gestures and an accuracy of 98.5% with a group of six pinch gestures. The proposed method realized a higher accuracy in pinch gesture set while using fewer electrodes. Additionally, we designed two real-time proof-of-concept interactive scenarios to demonstrate the general applications of this system.

1. Introduction

Human-computer interaction (HCI) is a research field focusing on the design and development of interfaces between people and computers. Traditional interaction methods such as mice, keyboards and touchpads are lacking intelligence and convenience for users. Thus, a more natural and intelligent approach is required. The gesture recognition plays an important role in HCI and is one of the most convenient and effective methods. Therefore, many applications in gesture recognition systems have been explored. For example, at-home rehabilitation for individuals with hand disabilities and remotely controlling a home service robot [1, 2]. According to the forms of perception, the gesture recognition can be divided into two categories: non-touch sensing, and on-body sensing.

Non-touch methods have been proposed for hand-pose recognition by using either radio-frequency signals [3–5], or camera-based sensing information [6,7]. For example, Taylor et al. [8] used depth cameras to capture gesture data and applied machine learning methods to achieve a gesture recognition system for real-time tracking. Lien et al. [3] developed a device called Soli, which is a miniature radar that can be leveraged for real-time motion tracking of the human hand. Later they applied this radio-frequency signal to recognize 11 dynamic gestures

based on a deep learning algorithm [5]. Although these methods provide a rich means of gesture recognition, they rely heavily on environment-mounted sensors or body-worn devices. Therefore, the issues with occlusions for camera-based sensing and the frequency interference in the air for the radio-frequency signals may limit user mobility.

Compared with the non-touch sensing, the on-body sensing has shown more promise for real-time gesture recognition [9–12]. For example, Yubaiz et al. proposed a wearable glove-based Arabic sign language recognition system with two DG5-VHand data gloves to capture hand movements, and achieved a sentence recognition rate of 98.9% [10]. Chang et al. introduced a sensor glove that can monitor and capture hand motion by using a novel inertial sensor fusion control algorithm to process 3-D real-time measurement data [11]. However, glove-based sensing approaches require delicate instrumentation on the user's fingers and palm, which are complex and expensive. Rossi et al. adopted electromyographic (EMG) as input signals and proposed a hybrid classifier based on support vector machines and a hidden Markov model for gesture recognition [13]. However, the EMG sensor failed to capture fine finger motion and large-scale motion. Delpreto et al. used inertial motion unit (IMU) sensor in wearable device which enables a plug-and-play detection of four types of gestures [14]. The IMU sensor

* This paper was recommended for publication by Associate Editor Prof. Micky Rakotondrabe

* Corresponding author.

E-mail address: xjwang@iamt.ac.cn (X. Wang).

can detect movements and reconstruct motion trajectories by measuring the rotational and acceleration speed information. The disadvantages of this sensor lies in its much noise and low sensitivity to small-scale motion.

The application of electrical impedance tomography (EIT) technology for gesture recognition has attracted much research interest [15,16]. EIT is a non-invasive imaging technique that can detect the interior structural impedance distribution of a conductive object. By analyzing the impedance measurements from the surface electrodes surrounding the subject, the inner impedance distribution can be monitored graphically in real time [17]. Since the bones and muscles within the wrist show different statuses for various gestures that can be distinguished by interior impedance distribution [15]. Therefore, the EIT technology can be employed to recognize hand gestures [18–20].

Similar to the EMG sensor, the EIT sensor need electrodes attached to the skin surface for gesture recognition. The difference between them is that the latter is required alternatively exciting a pair of electrodes to obtain impedance data from other electrodes. In this case, the signal of the EIT sensor is easier to identify than other bioelectrical signals. However, a typical EIT-based hand gesture recognition system usually requires multiple electrodes (8 or more) wrapped around the wrist, which is not convenient for wearable devices. For example, Zhang et al. proposed Tomo [15], which used an 8-electrode system to detect the cross-sectional impedance of the wrist for recognizing hand gestures and later upgraded to 16 and 32 electrodes with a constant frequency of 40 kHz [20]. Yao et al. proposed a wearable EIT sensor with 8 electrodes for gesture recognition and explored the performance when using electrodes of different materials and shapes [19]. Jiang et al. reported a 16-electrode EIT system by changing the electrode arrangement to measure 3D muscle contraction [21]. Atitallah et al. proposed an EIT system with 8 electrodes for gestures recognition, and achieved an accuracy of 95.94% using convolutional neural network (CNN) classification algorithm [22]. In our previous work we found that when EIT technology was adapted to gesture recognition, we can address this issue in classification rather than image reconstruction [23]. We achieved an acceptable accuracy of gesture recognition through feature extraction and model training, while ignoring the imaging process. Later, we proposed a bio-impedance analysis method (BIAM) with fewer electrodes [24] to improve the accuracy of gesture recognition by analyzing human hand anatomy and optimize the electrode positons. These methods can reduce the complexity of EIT-based gesture recognition systems; however, at least five electrodes are still needed in order to acquire bio-impedance signals appropriately. Most of all, previous work for EIT based gesture recognition devices employed the stimulus signal with a constant frequency would loss the frequency-dependent features of bio-impedance data, resulting in more disturbances in collected impedance data. A frequency difference EIT method (FD-EIT) has been proposed to consider the impedance distribution by collecting impedance data in several specific frequencies [25,26]. However, this method is applied for image reconstruction which is time-consuming and complicated. The reason is that not only the response data of the electrodes needs to be collected sequentially, but also different excitation signals need to be applied in sequence.

Considering that we can exploit the features of impedance data for gesture recognition without imaging, we might be able to take advantage of the FD-EIT approach by avoiding the image reconstruction procedure. In this study, we proposed a novel two-electrode frequency-scan system for gesture recognition based on bio-impedance measurement. First, the frequency-scan method was adapted to design a custom data acquisition circuit, which can generate safe electrical signals ranging from 20 kHz to 60 kHz. Then through feature extraction methods and machine learning classification models, we explored the relations between the gestures and impedance data under different frequencies. Last, we carried out a series of real-time gesture recognition tests to demonstrate proof-of-concept.

2. Methodology

The proposed method aims to achieve fast, accurate, and convenient gesture recognition, which consists of a wearable data acquisition device and an interaction application program. In Fig. 1, we describe the overall structure of the gesture recognition system. Two measurement electrodes were attached to the hand, and the frequency-scan method was used to collect bio-impedance data. Sinusoidal electrical signals are injected into one of the two electrodes and form a path through the other electrode. The response electrical signals generated from the two electrodes are collected by the homemade data acquisition board simultaneously. Then, the collected data are sent to a PC processor through wireless communication. In this section, we first described the sensing principle of the proposed gesture recognition system. Then we introduced the design of the data acquisition board and its implementation of frequency-scan method. Finally, we illustrated the feature extraction methods and the commonly classification methods.

2.1. Sensing principle

When we make different gestures, the internal structure of the palm, such as muscles and tendons, will show various statuses. The change in these statuses can be represented by bio-impedance variations [27]. The proposed sensing principle for hand gesture recognition is based on the measurement of the impedance distribution. In Fig. 2, we described the distribution of the musculature of the opisthenar, the equivalent circuit for bio-impedance measurement based on Cole-Cole model, and a schematic diagram of the electrode placement [28]. As shown in Fig. 2 (c), there are four slender lumbrical muscles connecting the four fingers outside the thumb. When we make different gestures, these lumbricals at the metacarpophalangeal joints would flex the fingers and extend the interphalangeal joints. The movement of the muscles can lead to changes in the impedance of the opisthenar. By applying a safe and controllable sinusoidal electric excitation signal and collecting the electrical response signal of the two electrodes, the impedance between the two electrodes can be obtained. Fig. 2(b) illustrates the equivalent model for impedance measurements, which consists of R_0 , R_1 and C_0 [28]. The calculation equation of equivalent impedance is shown as follows:

$$Z = R_1 + \frac{R_0 - R_1}{jwC_0(R_0 - R_1) + 1} \quad (1)$$

where R_1 means the low-frequency resistor and R_0 denotes the high-frequency resister. C_0 is an equivalent capacitor. w is the corresponding frequency. Compared with previous work of gesture recognition that a constant frequency is applied to multiple electrodes [16,20,24], we proposed a two-electrode frequency-scan method to reduce the number of electrodes. Although reducing electrodes results in a reduction in impedance data between different electrode pairs, the frequency-scan method can compensate the loss by adding frequency information. As shown in Fig. 2(a), we placed two medical electrodes on these lumbricals, and adopt the frequency-scan method to acquire the bio-impedance data for different hand gestures. One of the electrodes acted as the emitter, and the other served as the receiver. The commercial medical electrodes are composed of an Ag/AgCl electrode surrounded by a conductive gel. The gel is surrounded by an adhesive material, which is used to fix the electrodes. Therefore, the use of medical electrodes can ensure the surface electrodes are attached to the skin tightly so that the contact impedance between skin and electrodes are consistent for each test, making the measurement results more stable.

It should be noted that when we applied frequency-scan method for bio-impedance measurement, the excitation signal should conform to IEC 60,601 standards [29]. IEC 60,601 is a widely accepted series of technical standards for the basic safety and essential performance of

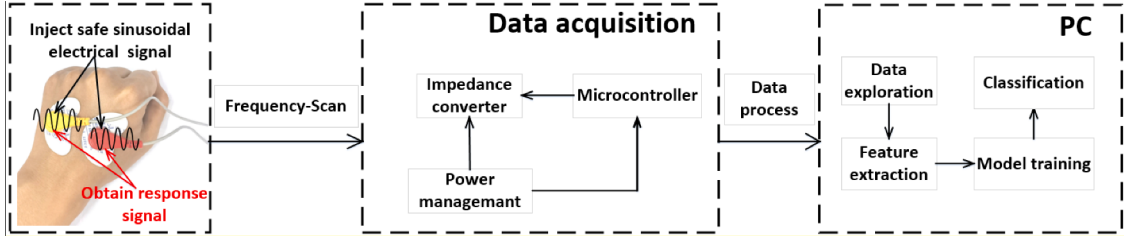


Fig. 1. The overall structures of the gesture recognition system.

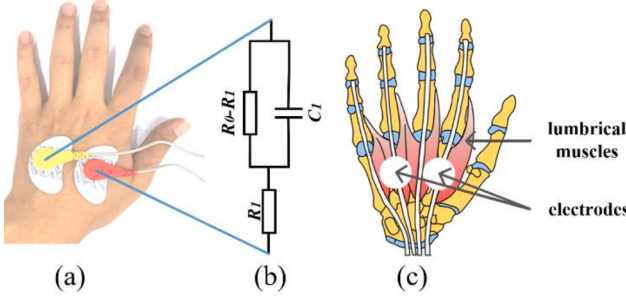


Fig. 2. Measurement prototype. (a) Electrodes placement (b) Equivalent model for impedance measurement (c) Lumbricals distribution (Palmar views).

medical electrical equipment. IEC 60,601 defines that for alternating current with a frequency component greater than 1 kHz, the value of current must not exceed 10 μ A. The value of the safe current increases with the increase of frequency. A typical current value that is safe to human for a device with frequency of 50 kHz should not be higher than 500 μ A. Once this standard is exceeded, the excitation signal will be harmful to the human body. Considering that a constant 40 kHz frequency with multiple electrodes can generate better data differences for gesture recognition [15], the frequency range in this paper also includes this common choice. Considering that the frequency reduction will lead to a smaller AC current that the human body can withstand, and the response signal must be sufficiently obvious for sampling, the excitation frequency of the signal should be in a reasonable range. Therefore, we set the frequency range from 20 kHz (allowable AC current 200 μ A at 20 kHz) to 60 kHz to obtain impedance data from the opisthenar and a step size of 2 kHz was adopted in this frequency-scan method.

2.2. Data acquisition board (frequency-scan method)

As shown in Fig. 3(a), we designed a bio-impedance measurement schematic based on the AD 5933 chip that can generate signals from 0 Hz to 100 kHz. Fig. 3(b) details the data acquisition board, which consists of a wireless Bluetooth module, a signal excitation module, a signal measurement module, and a control module. The AD5933 is an impedance converter chip that integrates a precision on-board frequency generator and a 12-bit, 1MSPS, analog-to-digital converter (ADC). The frequency generator applies a known frequency to the external complex impedance. The response signal from the measured object is sampled by the ADC and processed by discrete Fourier transform (DFT) method. Measured result is recorded by a data-word (real part Z_r and imaginary part Z_i) at each setting frequency. The magnitude of the real and imaginary components of the DFT is given by the following formula:

$$\text{Magnitude} = \sqrt{Z_r^2 + Z_i^2} \quad (2)$$

It should be noted that Z_r and Z_i do not represent the resistance and reactance of the measured object. To calculate the magnitude of the impedance, we need to obtain a calibration of gain factor as follows:

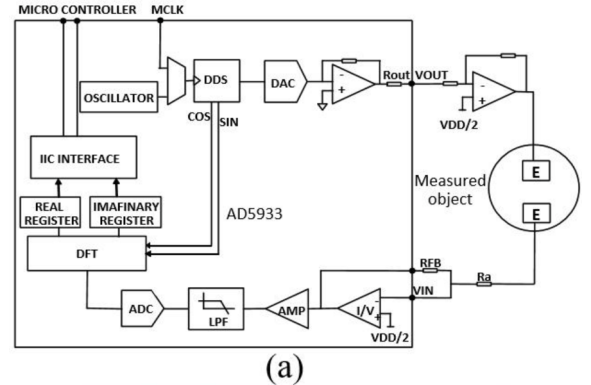


Fig. 3. (a) The circuit schematic of the board. (b) The data acquisition board.

$$|Z| = \frac{1}{\text{Gain} * \text{Magnitude}} \quad (3)$$

$$\text{Gain} = \frac{\text{Admittance}}{\text{Magnitude}} = \frac{\left(\frac{1}{\text{Impedance}}\right)}{\text{Magnitude}} \quad (4)$$

The gain factor is determined by using a known impedance ($2k\Omega$) between the two electrodes of the designed system and measuring the resulting magnitude of the resistance. In this paper, we obtained the magnitude of the impedance for subsequent calculations. As a programmable chip, AD5933 provides input interfaces for various frequency measurement methods. By setting the starting frequency, frequency increment and number of increments, the signal generator can work in a specific frequency-scan mode. The flowchart of frequency-scan method for impedance data collection is shown in Fig. 4. In this work, we performed bio-impedance measurement with excitation signals in the frequency range of 20 kHz to 60 kHz. To conform to IEC 60,601 standards and limit the amount of AC current entering the human body, we introduced a precision resistor (R_a). When calculating the R_a resistor value, the maximum output voltage from the AD5933 is 1.98 Vp-p (0.7000 Vrms). Setting the maximum allowable AC current to 80% of the maximum, or $160\mu\text{A}$, we can obtain the R_a resistor value

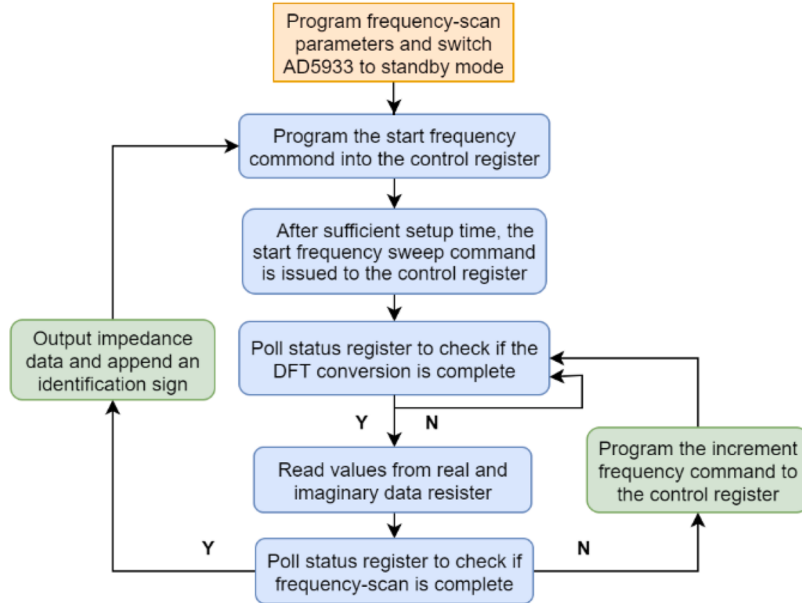


Fig. 4. The flowchart of frequency-scan method for impedance data collection.

using the following equation:

$$Ra = \frac{0.7000V_{rms}}{160\mu A_{rms}} = 4375\Omega$$

A \$5k\\$\Omega\$ Ra is selected and connected to the Vin pin of AD5933. Thus, we can ensure that the AC current is within the safe range. Since the signal generator will allow DC bias current to enter the measured object, which is harmful to the human body. We introduced a high-pass filter to remove the DC bias component from the voltage output of AD5933. When two electrodes were placed on the back of the hand, excitation signals were generated from the data acquisition board. The response signals from the electrodes were collected simultaneously, and the data were sent to a PC for further preprocessing. The acquisition process is repeated until a termination signal is received. Since the data collection process of the system is real-time and continuous, in order to accelerate the process of subsequent data analysis, we added an identification segmentation symbol after each frequency scan was completed. Therefore, when we received and divided gesture data according to different frequencies, we only needed to detect the separator to complete the segmentation, which would accelerate the data processing.

2.3. Data analysis

The bio-impedance data from the opisthenar was obtained using the two-electrode frequency-scan data acquisition board. Considering that there may be some ambient noise in the collected data, we adopted threshold filtering and average filtering methods to preprocess these data. Since the frequency interval is chosen to be 2 kHz, the original impedance data dimension is twenty-one. According to previous studies, we exploited the distribution characteristics of impedance data under different gestures. The Euclidean distance of the impedance data under the same gesture will be small, while it will increase under different gestures. Therefore, these impedance data will be input into the training model as representational features for gesture recognition.

To achieve high-accuracy gesture recognition, we explored the relationship between impedance data and gesture recognition, and constructed multiple statistical features to characterize the impedance data. As we perform different gestures, the bio-impedance of the opisthenar will change accordingly. The value of impedance data will show different distribution characteristics under different frequency mea-

surements. Therefore, we explored the statistical dispersion of bio-impedance data under different gestures, and introduced the coefficient of variation (COV) to measures the change level of impedance data. The COV is given by:

$$COV = \frac{\sigma}{\mu} = \frac{\sqrt{N * \sum_{n=1}^N (x_n - \mu)^2}}{\sum_{n=1}^N x_n}, \mu = \frac{1}{N} \sum_{n=1}^N x_n \quad (5)$$

where x_n represents the impedance data of a single gesture, N is the number of samples in a single gesture, μ and σ denote the mean and stand deviation of impedance data, respectively. Then, we used the characteristics of the frequency-scan method to construct a first-order difference feature: $\Delta x(n) = x(n+1) - x(n)$, which represents the change speed of the impedance data when the injection frequency increases linearly. Since the impedance data under the same gesture is related to the frequency change, we constructed the first-order autocorrelation (FAC) of the impedance value with the frequency change, and introduced its calculation form:

$$FAC = \frac{1}{(N-1)\sigma^2} \sum_{n=1}^{N-1} (x_n - \mu)(x_{n+1} - \mu) \quad (6)$$

In addition, the collected impedance data were processed through the normalization method as it can improve the convergence speed of the classification model. Since the accuracy of gesture recognition system not only depends on the acquisition and preprocessing of data in hardware, but also depends on the classification algorithms in software; we selected six commonly used algorithms for classification model training and compared their training time and accuracy. The six algorithms are support vector machine (SVM) with a radial basis function (RBF) kernel, multinomial naive Bayes (NB), K-nearest neighbor (KNN), logistic regression (LR), random forest (RF), and Adaboost. To quickly realize these classifiers in the experiments, we used the Python module Scikit-learn [30] as a machine learning library.

3. Experiments and results

In this section, we described the experimental procedure and analyzed the results of the proposed method for gesture recognition. In accordance with previous work [15,24], we chose nine gestures and divided them into two gesture sets. One is pinch gesture set that is designed for fine hand gesture recognition. The other is a common

gesture set for rough hand gesture recognition. Seven participants (five males, two females) ranging in age from 20 to 35 years were recruited for data collection. Six of the participants were right-handed and one was left-handed. Participants' hand length ranged from 17.5 cm to 20.5 cm. They are all in good health and two of them are regular exercisers. According to the previous data processing method, we processed the data of the two gesture sets and trained classification models for gesture recognition. In addition, a conceptual real-time gesture recognition experiment was conducted to prove the accuracy of the method, and the recognition results were used to control the dexterous hand for interaction, which demonstrated its potential for practical application.

3.1. Pinch gestures

Six pinch gestures including thumb press, middle pinch, index pinch, ring pinch, and spider-man were designed to conduct this experiment. Before conducting this experiment, participants need to maintain a comfortable sitting position and practice hand gestures. Then, two medical electrodes were placed on the selected locations of the participant's hand. When data collection started, 20 samples were recorded for each gesture, and different gesture measurements were carried out until all five gestures were finished. Five repeated cycles were performed for each participant. The entire experiment took approximately two hours, and a total of 4200 samples were acquired. Fig. 5(a) describes the six gestures whose names are A-1 to A-6, and Fig. 5(b) shows the impedance distribution of this gesture data. As the frequency increase, the impedance data will decrease. We selected the features fea_1 and fea_2 at the first two frequencies to explore the relationship characteristics of data changing with gestures. As shown in Fig. 5(c), the impedance data under six pinch gestures show the intra-class clustering characteristics and inter-class distinguishability. In addition, we can see that bio-impedance of the six gestures have different distributions with frequency.

During the training of classification models, a five-fold cross-

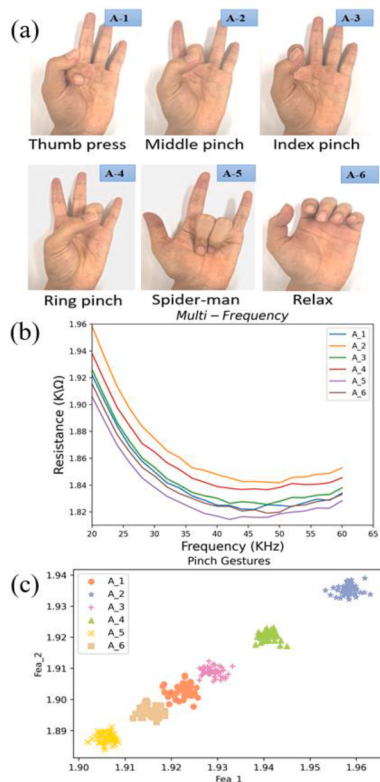


Fig. 5. Pinch gesture set. (a) Six pinch gestures. (b) Six typical impedance distributions of the gesture set as a function of frequency. (c) Clustering characteristics of impedance data under six pinch gestures.

validation method was adopted to avoid overfitting. Five-fold means that the original data was divided into five subsets and one of them is the validation set in turn. Therefore, one cycle of the collected data was used as the validation set, and the other cycles were used as the training set. Through feature extraction, forty-three represent features were input to classification models for training. In Table 1, we detailed the recognition accuracy, training time and running time of pinch gestures under six classification models. From the table, we can see that selecting different recognition algorithms will have different training time, recognition accuracy and speed. All recognition algorithms can complete recognition within 5 ms, and the recognition accuracy of all algorithms can reach more than 91%. We compared the training time of these classification models and found that the NB algorithm has the shortest training time about 0.32 s and the LR algorithm has the longest training time about 7.35 s. In contrast, the RF algorithm with the highest accuracy took only 1.63 s. Among them, the KNN method has the lowest recognition accuracy of 91.7%. Interestingly, for the LR algorithm, it spends the longest training time while has the fastest recognition speed of 0.53 ms. Although the RF algorithm has the longest running time of 4.48 ms, it achieves the highest recognition accuracy of 98.5%. For the pinch gesture set, previous work [18] using EIT based 8-electrode single frequency method combined with artificial neural network algorithm achieved a maximum accuracy of 92%. The BIAM system using 5-electrode single frequency method with SVM algorithm achieved an accuracy of 97.8% [24]. However, the proposed frequency-scan two-electrode system with RF algorithm can achieve much better results in pinch gesture recognition with only two electrodes. The reasons can be explained as follows.

The first is due to the locations of the electrodes installed. According to the distribution of the wrist muscles, we attached the electrodes to the lumbricals, which is related to the bending of the fingers, so that the collected data is sensitive to the movement state of the fingers. The second is that [18] did not explore the characteristics of bio-impedance data, and they used ANN algorithm with only one hidden layer for classification, which cannot capture representative features for different gestures. The last might be the impedance signals obtained with the frequency-scan method could increase the frequency characteristics of data. In comparisons with the data acquisition system with fixed frequency method, it is beneficial to distinguish different gestures.

3.2. Common gestures

In this experiment, we designed four common gestures to further illustrate the effectiveness of the proposed method. The gesture set included stretch, fist, relax, and thumbs up, which are commonly used in daily life. We named these gestures B-1 to B-4 for convenience and conducted five circles to collect gesture data. After completing the experiment according to the above procedure, we collected 2800 samples from the opisthenar. Fig. 6 shows the gesture set and the trend of the bio-impedance data with frequency. Similar to pinch gestures, we draw the impedance data under four gestures with the intra-class clustering characteristics and inter-class distinguishability in Fig. 6(c). It can be seen that the bio-impedance data show the clustering characteristics which are good for feature selections.

Five-fold cross-validation method was adopted to train and validate

Table 1

Performance comparison of pinch gesture set of six classification models.

Algorithms	Pinch gestures	Training Time (s)	Running time (ms)
SVM	0.961	0.65	0.93
NB	0.957	0.32	0.65
RF	0.985	1.63	4.48
KNN	0.917	0.92	2.91
LR	0.925	7.35	0.53
Ada	0.958	1.64	1.35

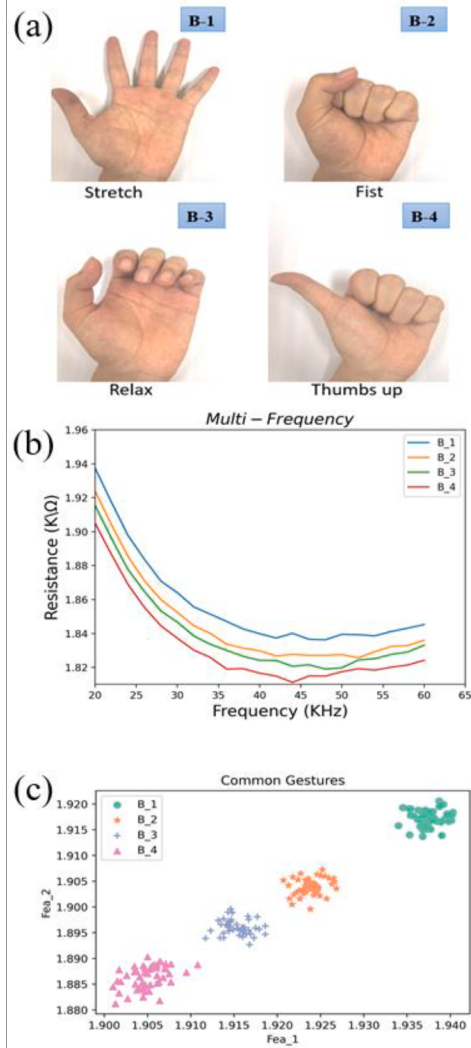


Fig. 6. Common gesture set. (a) Four hand gestures. (b) Four typical impedance distributions of the gesture set as a function of frequency. (c) Clustering characteristics of impedance data under four common gestures.

the classification models. Table 2 lists the performance comparison of common gesture set for six classification models. From the table we can find that the training time of the common gesture set for each model is similar to pinch gesture set. The LR algorithm took more time to train the classification model while achieved faster gesture recognition. The training time of NB algorithm was lesser than others as it took about 0.12 s. Among the six algorithms, RF and Ada achieved highest recognition accuracy of 98.3%. However, Ada algorithm took lesser running time than RF. Compared with the EIT system that using 8-electrode single frequency method for common gestures recognition [18], our frequency-scan two-electrode method achieved a higher recognition accuracy. In addition, we find that the accuracy of the KNN algorithm is different under the two recognition methods. Similarly, SVM algorithm

behaves differently in the two recognition methods. This is because the electrode positions and frequency patterns of the two methods are different, resulting in different distributions of the obtained datasets.

3.3. Real-time gesture recognition

We list the confusion matrices of the recognition results for the two gesture sets in Fig. 7 and explore the recognition accuracy for different gestures. In the confusion matrix, the label of horizontal axes represents the index of the predicted gesture, and the label of vertical axes is the index of the true gesture. The number in the small box of the diagram shows the ratio of the predicted gesture with the true gesture to the total number of samples of the gesture, and the sum of the numbers in each row is equal to 1. From these two pictures we find that the relax gesture has the lowest recognition accuracy, while most other gestures have reached more than 98%. According to the experimental analysis, fingers will show various degrees of bending for each participant when we relax our hand, which will cause enormous differences and make recognition difficult.

We carried out an interactive control experiment to demonstrate the real-time performance and accuracy of the gesture recognition system. The experiment consisted of two parts. The first is to obtain the impedance data of the palm through the proposed gesture recognition system and analyze the data. The second part is to show the corresponding pictures according to the real-time recognition results. As shown in Fig. 8, when we changed the gestures, the system recognized the hand motion and the PC displayed different gestures. The experimental results indicated that the gesture recognition system can be effectively applied to human-computer interaction (HCI) (details can be seen in the video ‘hand gesture demons’).

To further illustrate the practicability of the gesture recognition system, we conducted an experiment of controlling the dexterous hand. We introduced a dexterous hand (RH56DF3-1R, Inspire-robots Inc., China) that integrated six micro linear actuators and five sensitive pressure sensors, as shown in Fig. 9. The dexterous hand has the characteristics of real-time detection of contact force and quick response to change gestures according to instructions. Through the RS232 serial communication protocol, the PC can send instructions to realize real-time control of the dexterous hand, such as completing some grasping and pre-set actions. In addition, the response time of the dexterous hand can be adjusted according to the requirement of the experiment, and its range is from 0 to 1000 ms. We adopted the default setting response time of the dexterous hand (500 ms). Simultaneously, the dexterous hand can feed back the contact force and the status of the gestures to the PC. In this experiment, the goal is to use the two-electrode, frequency-scan gesture recognition system to recognize the hand gesture, and encode the recognition result as instruction to control the dexterous hand to reproduce the same gesture. At first, we placed two electrodes on the back of our hand to collect the impedance data, and sent the data to PC by Bluetooth. Then, the representative features were constructed and input to classification model to get the recognition result. Next, control instructions were encoded according to the result, and sent to the dexterous hand by RS232. Lastly, the dexterous hand will do the same gesture and feed back the contact force to the PC once it received instructions. Real-time interaction with dexterous hand were shown in Fig. 9 (details in the video ‘hand gesture demons’).

4. Conclusion

We designed a two-electrode frequency-scan gesture recognition system based on bio-impedance and conducted two groups of gestures to verify the effectiveness and availability of the proposed system. Compared to previous work, we significantly simplified the complexity of the gesture recognition system, while achieving a high recognition accuracy. Through frequency-scan method and feature extraction method, we explored and constructed representative features for gesture

Table 2

Performance comparison of common gesture set of six classification models.

Algorithms	Common gestures	Training Time (s)	Running time (ms)
SVM	0.972	0.43	0.95
NB	0.975	0.12	0.63
RF	0.983	0.99	4.57
KNN	0.916	0.64	2.88
LR	0.955	5.27	0.49
Ada	0.983	1.12	1.41

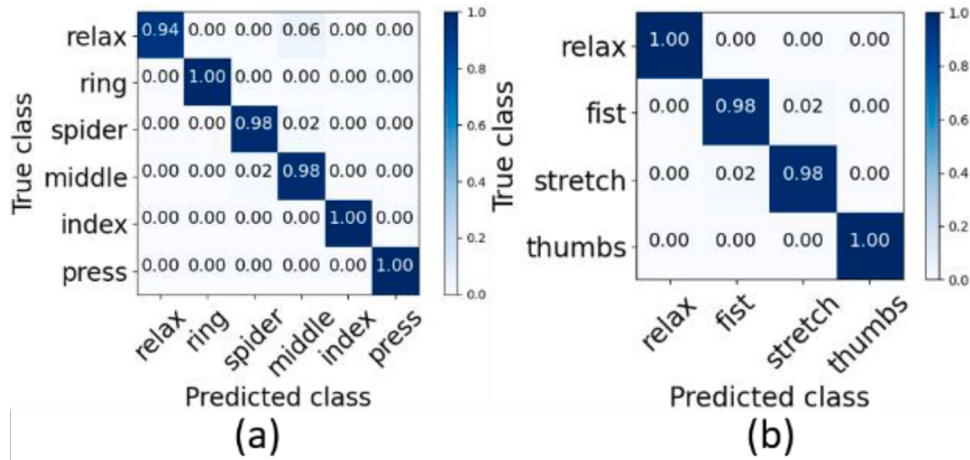


Fig. 7. Confusion matrix of two hand gesture sets using RF classifier. (a) pinch gestures (b) common gestures.

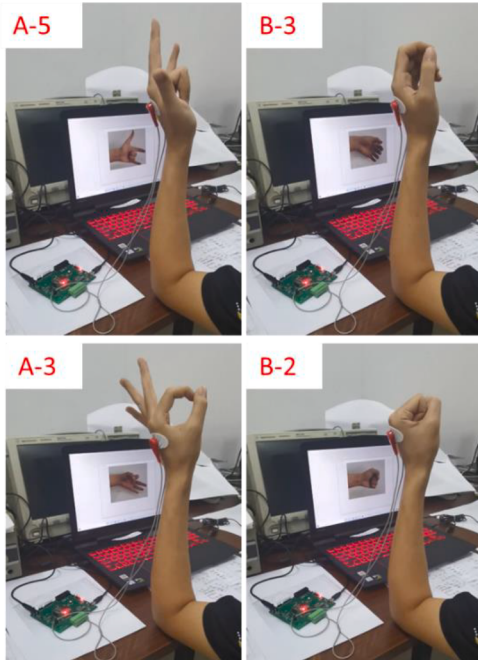


Fig. 8. The recognized gestures were encoded to control the laptop to show different pictures.

recognition. In pinch gesture set experiment, we introduced six finger-bending gestures and achieved a recognition accuracy of 98.5% with two electrodes. The results show that this method has more advantages than EIT and BIAM method (previous work using constant single frequency multiple electrodes) in recognition pinch gestures, as it realized a higher accuracy while using less electrodes. In common gesture set experiment, the proposed system achieved a recognition accuracy of 98.3% when detecting four common gestures. To better explain the practicability and general purpose of the system, two proof-of-concept and real-time interactive scenarios were performed. In future work, we will further explore more repeatable electrodes instead of medical electrodes, and simplify the hardware design of the gesture recognition system to make it more portable. We will also continue to investigate gesture data structures to obtain more robust features for gesture recognition.

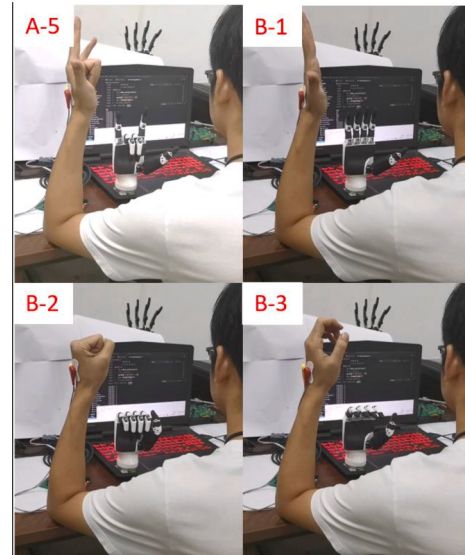


Fig. 9. Manipulator interaction application. The recognized gestures were used to control the manipulator.

CRediT authorship contribution statement

All authors contributed to the study conception and experimental evaluations. Hardware design was performed by [Gang Ma] and [Hao-feng Chen], data analysis was completed by [Gang Ma] and [Peng Wang], and experimental tests were performed by [Shuai Dong] and [Gang Ma]. The first draft of the manuscript was written by [Gang Ma], and reviewed and revised by [Xiaojie Wang]. Supervision and Funding acquisition were carried out by [Xiaojie Wang] and [Shuai Dong]. All authors commented on previous versions of the manuscript, and all read and approved the final manuscript.

Declaration of Competing Interest

The authors declare that they have no known competing financial interests or personal relationships that could have appeared to influence the work reported in this paper.

Data availability

Data will be made available on request.

Acknowledgments

This work is supported by the Anhui Provincial Nature Science Foundation (Grant No.2008085QE253) and the Key Support Project of Dean Fund of Hefei Institutes of Physical Science, CAS, under Grant YZJJZX202017).

Supplementary materials

Supplementary material associated with this article can be found, in the online version, at [doi:10.1016/j.mechatronics.2023.103039](https://doi.org/10.1016/j.mechatronics.2023.103039).

References

- [1] Polygerinos P, Wang Z, Galloway KC, Wood RJ, Walsh CJ. Soft robotic glove for combined assistance and at-home rehabilitation. *Rob Auton Syst* 2015;73:135–43.
- [2] Yu N, Xu C, Wang K, Yang Z, Liu J. Gesture-based telemanipulation of a humanoid robot for home service tasks. In: 2015 IEEE international conference on cyber technology in automation, control, and intelligent systems (CYBER). IEEE; 2015. p. 1923–7.
- [3] Lien J, et al. Soli: ubiquitous gesture sensing with millimeter wave radar. *ACM Trans Graphics (TOG)* 2016;35(4):1–19.
- [4] Abdelnasser H, Harras K, Youssef M. A ubiquitous WiFi-based fine-grained gesture recognition system. *IEEE Trans Mobile Comput* 2018;18(11):2474–87.
- [5] Wang S, Song J, Lien J, Poupyrev I, Hilliges O. Interacting with soli: exploring fine-grained dynamic gesture recognition in the radio-frequency spectrum. In: Proceedings of the 29th annual symposium on user interface software and technology; 2016. p. 851–60.
- [6] Weichert F, Bachmann D, Rudak B, Fisseler D. Analysis of the accuracy and robustness of the leap motion controller. *Sensors* 2013;13(5):6380–93.
- [7] Zhu G, Zhang L, Shen P, Song J, Shah SAA, Bennamoun M. Continuous gesture segmentation and recognition using 3dcnn and convolutional lstm. *IEEE Trans Multimedia* 2018;21(4):1011–21.
- [8] Taylor J, et al. Efficient and precise interactive hand tracking through joint, continuous optimization of pose and correspondences. *ACM Trans Graphics (TOG)* 2016;35(4):1–12.
- [9] Tubaiz N, Shanableh T, Assaleh K. Glove-based continuous Arabic sign language recognition in user-dependent mode. *IEEE Trans Hum Mach Syst* 2015;45(4):526–33.
- [10] Pławiak P, Sośnicki T, Niedźwiecki M, Tabor Z, Rzecki K. Hand body language gesture recognition based on signals from specialized glove and machine learning algorithms. *IEEE Trans Ind Inf* 2016;12(3):1104–13.
- [11] Chang HT, Chang JY. Sensor glove based on novel inertial sensor fusion control algorithm for 3-D real-time hand gestures measurements. *IEEE Trans Ind Electron* 2019;67(1):658–66.
- [12] Shatilov K, Kwon YD, Lee LH, Chatzopoulos D, Hui P. MyoKey: inertial motion sensing and gesture-based QWERTY keyboard for extended realities. *IEEE Trans Mobile Comput* 2022.
- [13] Rossi M, Benatti S, Farella E, Benini L. Hybrid EMG classifier based on HMM and SVM for hand gesture recognition in prosthetics. In: 2015 IEEE international conference on industrial technology (ICIT). IEEE; 2015. p. 1700–5.
- [14] DelPreto J, Rue D. Plug-and-play gesture control using muscle and motion sensors. In: Proceedings of the 2020 ACM/IEEE international conference on human-robot interaction; 2020. p. 439–48.
- [15] Zhang Y, Harrison C. Tomo: wearable, low-cost electrical impedance tomography for hand gesture recognition. In: Proceedings of the 28th annual ACM symposium on user interface software & technology; 2015. p. 167–73.
- [16] Lu X, Sun S, Liu K, Sun J, Xu L. Development of a Wearable Gesture Recognition System Based on Two-terminal Electrical Impedance Tomography. *IEEE J Biomed Health Inform* 2021.
- [17] Bayford RH. Bioimpedance tomography (electrical impedance tomography). *Annu Rev Biomed Eng* 2006;8:63–91.
- [18] Wu Y, Jiang D, Liu X, Bayford R, Demosthenous A. A human-machine interface using electrical impedance tomography for hand prosthesis control. *IEEE Trans Biomed Circuits Syst* 2018;12(6):1322–33.
- [19] Yao J, et al. Development of a wearable electrical impedance tomographic sensor for gesture recognition with machine learning. *IEEE J Biomed Health Inform* 2019.
- [20] Yang Z, Xiao R, Harrison C. Advancing hand gesture recognition with high resolution electrical impedance tomography. In: The 29th annual symposium; 2016.
- [21] Zhang K, Li M, Yang F, Xu S, Abubakar A. Three-dimensional electrical impedance tomography with multiplicative regularization. *IEEE Trans Biomed Eng* 2019;66(9):2470–80.
- [22] Attallah BB, et al. Hand sign recognition system based on EIT imaging and robust CNN classification. *IEEE Sens J* 2021;22(2):1729–37.
- [23] Ma G, Hao Z, Wu X, Wang X. An optimal electrical impedance tomography drive pattern for human-computer interaction applications. *IEEE Trans Biomed Circuits Syst* Jun 2020;14(3):402–11. <https://doi.org/10.1109/TBCAS.2020.2967785>.
- [24] Chen H, Ma G, Wang P, Wang X. A bio-impedance analysis method (BIAM) based on human hand anatomy for hand gesture recognition. *IEEE Trans Instrum Meas* 2021. <https://doi.org/10.1109/tim.2021.3112775>. 1–1.
- [25] Rapin M, et al. Wearable sensors for frequency-multiplexed EIT and multilead ECG data acquisition. *IEEE Trans Biomed Eng* 2018;66(3):810–20.
- [26] McDermott BJ, Ohalloran M, Avery J, Porter E. Bi-frequency symmetry difference EIT-feasibility and limitations of application to stroke diagnosis. *IEEE J Biomed Health Inform* 2019.
- [27] Zhu J, et al. EIT-kit: an electrical impedance tomography toolkit for health and motion sensing. In: The 34th Annual ACM Symposium on User Interface Software and Technology; 2021. p. 400–13.
- [28] Cole KS, Cole RH. Dispersion and absorption in dielectrics I. Alternating current characteristics. *J Chem Phys* 1941;9(4):341–51.
- [29] Commission IE. Medical electrical equipment-Part 1: general requirements for basic safety and essential performance. IEC 2005. 60601-12005.
- [30] Pedregosa F, et al. Scikit-learn: machine learning in Python. *J Machine Learn Res* 2011;12:2825–30.



Xiaojie Wang received the B.S. degree in fluid mechanics from Tsinghua University, Beijing, China, in 1989, the M.S. degree in solid mechanics from the University of Science and Technology of China, Hefei, China, in 1998, and the Ph.D. degree from the Department of Mechanical Engineering, University of Nevada at Reno, Reno, NV, USA, in 2002. He was conducting research on intelligent materials and devices at the University of Nevada at Reno, for more than ten years. He is the Founder and currently the Director of the Bio-Inspired Robotics and Intelligent Material Laboratory, Institute of Advanced Manufacturing Technology, Chinese Academy of Sciences, Changzhou, China. He is also an Adjunct Professor with the University of Science and Technology of China, Hefei, China, and also an External Supervisor with the Faculty of Engineering and Information Technology, University of Technology Sydney, Ultimo, NSW, Australia. He has authored or coauthored more than 150 scientific publications with chapters in three books and holds six patents. His research interests include bio-inspired robots, smart materials, sensors/actuators, and mechatronic systems.